Efficient diode-pumped Er:YAP master-oscillator power-amplifier system for laser power improvement at 2920 nm

Efficient diode-pumped Er:YAP master-oscillator power-amplifier system for laser power improvement at 2920 nm

WEICHAO YAO,[1] ⓘ ENHAO LI,[2] ⓘ HIYORI UEHARA,[1,2] AND RYO YASUHARA[1,2,*] ⓘ

[1]*National Institute for Fusion Science, 322-6, Oroshi-cho, Toki 509-5292, Japan*
[2]*The Graduate University for Advanced Studies (SOKENDAI), 322-6, Oroshi-cho, Toki 509-5292, Japan*
[*]yasuhara@nifs.ac.jp

Abstract: We report on the first demonstration of laser-diode-pumped master-oscillator power-amplifier (MOPA) system based on Er-doped bulk material working at 2920 nm. The relaxation oscillation at the beginning of the laser pulse from the Er:YAlO$_3$ (YAP) oscillator was suppressed effectively when the pump frequency was increased to 140 Hz, as a result of the establishment of a three-level system. In the amplifier, the small signal gain of the Er:YAP strongly depends on pump duration and repetition frequency, and can reach the upper limit of parasitic oscillation. Further, 25.5 mJ of output pulse energy has been achieved from the amplifier at 150 Hz frequency (2.2 ms pump duration), with over 32% of optical-to-optical efficiency. Further improvement of the amplification ability of the MOPA system was discussed.

1. Introduction

Er^{3+}-doped lasers emitting in the mid-infrared spectral region (~3 μm) have increasingly become the forefront research topic for environmental monitoring, remote sensing [1], and some surgical applications [2] because they can effectively cover the absorption lines of many molecules [3]. It is expected that the 3 μm Er^{3+}-doped lasers may be applied in the industry specially for the processing of some hard and brittle glasses and flexible resin materials, benefitting from the strong stretching absorption of OH and C–H bonds [4,5]. To date, the demand for power enhancement of 3 μm laser is continuing to increase considering these potential applications [6], and scaling mid-infrared lasers to high-average power or high-energy levels have become one of the goals of current laser research [6–10].

In the recent years, laser-diode (LD)-pumped solid-state laser has shown the advantage of higher optical-to-optical conversion efficiency in the development of laser sources [9]. Similarly, the 3 μm Er laser that pumped by commercially available 976 nm LD also features a higher quantum efficiency via the energy-transfer up-conversion effect (ETU) between Er^{3+} ions [11,12]. However, even so, the LD-pumped Er laser often shows a relatively low conversion efficiency, e.g., ~30% [9,10], because of ~70% quantum defect. Further, the gain medium often has a high doping concentration (Er:YAG: 50 at.% [13], Er:YSGG: 35 at.% [8], Er:Lu$_2$O$_3$: 11 at.% [14]) to enhance the ETU effect. Despite that the continuous-wave (CW) laser operation can be obtained and the laser conversion efficiency has been greatly improved, strong thermal effect and the subsequent cavity instability and material damage are the main issues that limit the power improvement of the laser oscillator [9,10,12].

In contrast, master-oscillator power-amplifier (MOPA) system provides a simpler approach than developing an oscillator to achieve a higher output power. The heat induced by quantum defect can be dissipated by multi-stage amplifiers, which will greatly reduce the instability of the laser and the possibility of fracture damage of the gain medium. To date, MOPA systems based on Er:ZBLAN fiber have been successfully developed to achieve robust high-power

mid-infrared lasers [15–17]. Although Er:ZBLAN fiber MOPA system can provide efficient power amplification, the time domain and spectral distortion induced by nonlinear effects still can not be ignored under high-intensity condition [16,17]. In this case, MOPA system based on bulk Er^{3+}-doped materials is more attractive. However, thus far there are no reports on LD-pumped Er^{3+}-doped solid-state MOPA system working at 3 μm, except for only a few flash-lamp pumped Er:YAG MOPA systems [18,19]. Results show that flash-lamp pumped Er:YAG has a low laser gain [18,19]. Fortunately, it is possible to obtain higher laser gain via the LD end-pumping scheme because of enhanced ETU effect and easily controllable pump radius. Thus, considering the urgent needs of current applications, research on the amplification performance, e.g., the sing-pass small signal gain (SSG), power saturation and other issues that exist in the LD-pumped Er^{3+}-doped solid-state MOPA are becoming more and more significant.

Er:YAlO$_3$ (Er:YAP) crystal is a promising laser material for generating 2.92 μm laser benefitting from very low phonon energy and excellent physical properties [9]. The reported results from laser oscillators show that Er:YAP laser can provide more than 30% slope efficiency with 5 at.% doping concentration [9,20]. The relatively low doping concentration allows us to use a longer crystal, which is more beneficial for the amplifier. Thus, in this work we developed an LD-pumped Er:YAP MOPA system working in the mid-infrared spectral region. With a seed injection provided by a quasi-continuous-wave (QCW) Er:YAP oscillator, 32.3% of optical-to-optical (O-O) efficiency was successfully achieved from the amplifier.

2. Experimental setup

The LD-pumped MOPA system consists of a QCW Er:YAP oscillator and a single-pass Er:YAP amplifier, as shown in Fig. 1. The laser oscillator was composed of a plane input mirror (IM, T>95% at 960~980 nm, R>99% at 2.6~3 μm) and a plane output coupler (OC, T_{OC} = 2.5% at 2.8~3 μm). A *b*-cut 5 at.% Er:YAP crystal (space group: *Pbnm*) with a cross-section of 2 mm×5 mm and a length of 8 mm was used as the gain medium. The two surfaces of the crystal were polished without any coating. To reduce the loss induced by the vapor in the air, the cavity was adjusted to as short as possible, resulting in a cavity length of ~14 mm. The pump light was provided by a fiber-coupled and wavelength-unstabilized 976 nm LD with a fiber core diameter of 105 μm and a numerical aperture (NA) of 0.22. The core of the fiber was imaged in the crystal to a diameter of 350 μm via a 3:10 telescope system (L1: *f* = 30 mm, L2: *f* = 100 mm). Some residual pump light remained behind the OC was blocked by a band-pass filter (2.5–3.1 μm). Detailed parameters of the oscillator can be found in our previous work [9].

Due to the anisotropic property of the Er:YAP crystal, linearly polarized laser (***E***//*a*) should be obtained directly from the oscillator [21]. Sapphire substrate of OC will introduce additional birefringence so as to change the polarization state of the output laser to elliptical polarization. Thus, a polarizer was placed behind the oscillator to obtain linearly polarized seed light. In the amplifier stage, a longer *b*-cut 5 at.% Er:YAP crystal (without any coating), i.e., 12 mm length was employed, which was considered to provide a higher SSG than a short crystal. The *a*-axis of the Er:YAP crystal was adjusted to be parallel to the polarization direction of the seed laser to achieve a higher gain. To reduce the possible power loss induced by vapor and optical elements, the total length of the MOPA system was designed as short as possible (~300 mm behind the OC), and only one lens (L3: *f* = 75 mm) as well as a dichroic mirror (DM, T>95% at 960~980 nm, R>92% at 2.8~3 μm) were used to focus and reflect the seed into the Er:YAP crystal. Pump light for the amplifier was provided by another fiber coupled and wavelength-unstabilized 976 nm LD (core diameter: 110 μm, NA: 0.15) with a better beam quality, and was collimated and thereafter focused into the Er:YAP crystal with a diameter of 330 μm by two lenses (L4: *f* = 50 mm, L5: *f* = 150 mm). According to our previous result [9], the use of wavelength-unstabilized LD will not have significant influence on the laser efficiency, except for the increase of single-pass absorption from ~50% (4 W pump peak power) to ~60% (50 W pump peak power) due to the
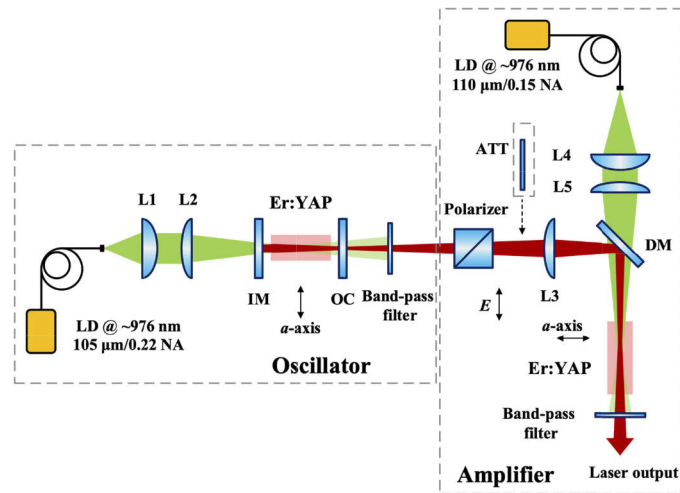
Fig. 1. Experimental setup of LD pumped Er:YAP MOPA system. The double-headed arrows indicate the *a*-axis of Er:YAP and laser polarization direction. NA: numerical aperture; IM: input mirror; OC: output coupler; L1-L5: lenses; ATT: attenuator; DM: dichroic mirror.

wavelength-shift of LD, measured directly without signal injection. Both of the Er:YAP crystals in the oscillator and the amplifier were mounted in copper holders and water-cooled to be 15 °C. The laser pulses were monitored using a PbSe amplified detector (PDA20H-EC, Thorlabs Corp.) with 10 kHz bandwidth and recorded by a 5 GHz oscilloscope (TDS5054B, Tektronix Corp.).

3. Results and discussions

3.1. Laser performance of QCW oscillator

First, the Er:YAP oscillator working in QCW mode was characterized at different repetition frequencies. Figure 2(a) shows the output performance of the oscillator when the pump duration was 1.5 ms at 28 W absorbed pump peak power. In this figure the pumping start time was marked as zero. We found that at a low frequency, i.e., 60 Hz, a giant pulse appeared at the beginning of the laser pulse, and only a slight part of other signals existed within the pump duration. When using a faster detector (C12492-210, Hamamatsu Photon. Corp.) to measure the giant pulse, we observed typical relaxation oscillations within this pulse. However, the giant pulse will gradually degrade with the increase of pump repetition frequency, and even be suppressed when the frequency was over 140 Hz. We think that the giant pulse was induced by the high gain provided by the four-level laser system at the beginning of laser oscillation. In this case, the laser wavelength should be located at the shorter wavelength (~2.7 μm) where the emission cross section is larger [14,22]. However, the laser will gradually transform into a three-level system when the pumping period approaches the radiative lifetime (~9.59 ms [20]) of $^4I_{13/2}$, and remain in a three-level system when the repetition frequency is beyond 140 Hz, since the pumping period was too short for the system to exhaust the excited ions on $^4I_{13/2}$ level. It should also be noted that at 140 Hz the laser pulse amplitude has reached the steady state for 1.5 ms pump duration, hence achieving stable laser wavelength because there is no large fluctuation in the waveform driven by wavelength jumping [23]. Therefore, we did not increase the pump duration any further. Then laser performance was characterized at 150 Hz frequency because the laser will be more stable working in a three-level system. A maximum average output power of 1 W can be obtained with a laser pulse width of 1.4 ms. The peak power was calculated to be ~5.6

W by normalizing the integrated waveform. The laser wavelength was measured by a spectrum analyzer (771B-MIR, Bristol Inst.), as shown in Fig. 2(b). A long-term averaged measurement shows that the laser wavelength was 2920 nm, and no other obvious wavelength signal can be observed. The relatively long wavelength confirms a three-level laser system.
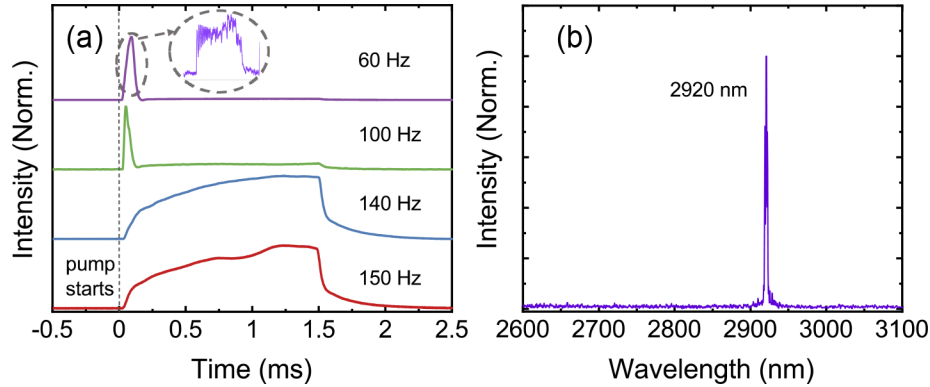

Fig. 2. Output characteristics of the QCW Er:YAP oscillator at 28 W absorbed pump peak power. (a) Normalized temporal waveforms at different frequency. Inset: relaxation oscillation pulses in the giant pulse; (b) Laser wavelength of Er:YAP oscillator at 150 Hz frequency.
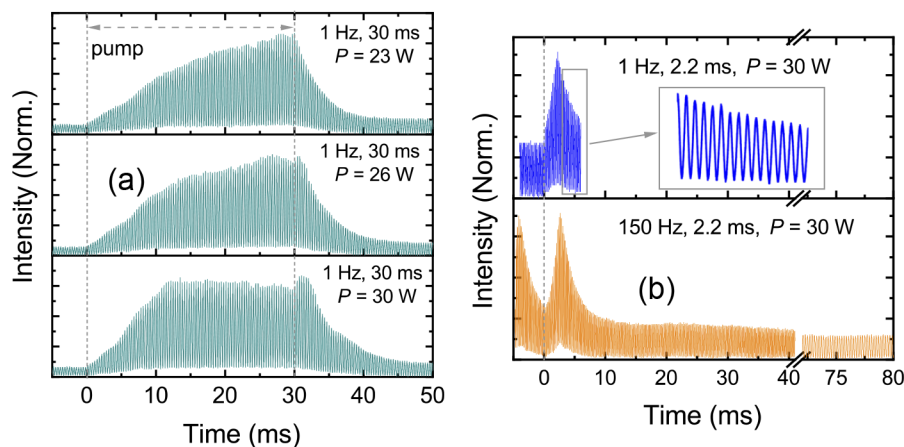
3.2. SSG measurement

Pump-probe method was used to measure the SSG of Er:YAP crystal in the amplifier. For this purpose, the oscillator was first operated in CW mode at the wavelength of 2920 nm. At 4.8 W absorbed pump power, the diameter of the signal laser was measured to be ∼300 μm by knife-edge method after it was focused by L3. In this case, excellent mode-matching between the pump and seed lights can be guaranteed. Approximately 10 mW signal power was incident into the crystal in the amplifier after the laser passed through an additional attenuator (ATT). Further, an optical chopper was used to modulate the output signal at 3 kHz or 5 kHz repeat frequency for the detection. The LD in the amplifier operated in QCW mode, and the SSG was determined by the amplitude ratio of the signal before and during the pump pulse that was measured by the PbSe detector.

Figure 3 shows the SSG measurement results under different pump duration and repetition frequency. At 1 Hz pump frequency, in addition to the exponential increase with increasing the absorbed pump peak power, the SSG also shows an obvious improvement with the pump duration extending from 2.2 ms (SSG = 2.9) to 10 ms (SSG = 10) at 30 W absorbed pump peak power. Due to the extremely short lifetime (0.85 ms) of $^4I_{11/2}$ level of Er:YAP crystal [20], the improvement of SSG with such a long pump duration is unlikely to be induced only by the population inversion excited by the pump source. Instead, we attributed the increase of SSG mostly to the ETU effect ($^4I_{13/2} + {}^4I_{13/2}$ $^4I_{15/2} + {}^4I_{9/2}$). Continuous ETU effect will promote the population inversion of the system [24]. Further, if the pumping duration was increased to 30 ms, SSG of the Er:YAP amplifier tends to be saturated when the absorbed pump peak power was beyond 23 W (SSG = 10.5). This type of saturation should be attributed to parasitic oscillation [25,26]. In this case, dimensionless parameter of g_0l can be estimated to be 2.35 (g_0 is SSG coefficient, l is crystal length). Theoretical calculation shows a parasitic oscillation limit value of $g_0l \approx 2.3$, according to the criteria $R_1R_2\exp(2g_0l) < 1$ [27], where $R_1 \approx R_2 \approx 0.1$ is the Fresnel reflectivity. The close values of theory and experiment are evidence of parasitic oscillation.
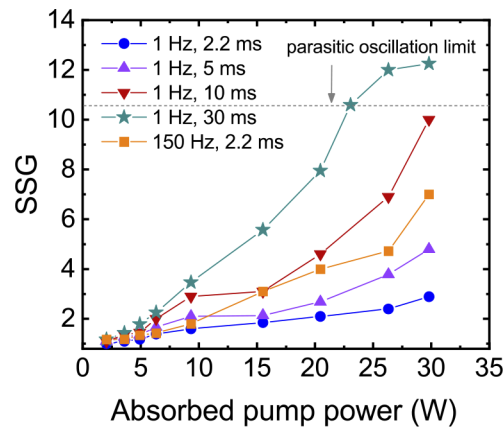
Fig. 3. SSG measurement under different pump duration and frequency.

Figure 4(a) shows the measurement waveforms at 1 Hz pump frequency and 30 ms pump duration under 23 W, 26 W, and 30 W absorbed pump peak power. Some non-modulated background in the waveform is related to the rising times of the chopper and the detector. However, even so the measured relative peak intensity is almost correct, hence ensuring the SSG measurement results. It can be seen that the SSG becomes higher with the pump time extending. In addition, the SSG will decline significantly when it reaches a certain value at 26 W and 30 W absorbed pump peak powers, which should be attributed to the rapid consumption of the populations on $^4I_{11/2}$ level induced by the parasitic oscillation. The slight increase of SSG after the pump duration is most likely induced by the ETU effect because the populations on $^4I_{13/2}$ level cannot be completely exhausted in a short time. Therefore, a lower absorbed pump peak power, i.e., 23 W was considered as the parasitic oscillation limited value in our experiment. It can be predicted that if the surface reflection of the Er:YAP crystal could be eliminated by anti-reflective coating, a higher SSG is still possible.


Fig. 4. Normalized measurement waveforms for SSG measurement. (a) SSG measurement results at 1 Hz frequency and 30 ms pump duration; (b) waveforms at 1 Hz and 150 Hz frequency, inset is zoom-in view of modulated signal in 3 ms.

Due to the limitation of current conditions, the amplifier cannot be synchronized with the QCW seed if the amplifier was designed under long pump duration and low repetition frequency, since

the seed oscillator works at 150 Hz repetition frequency. Meanwhile, increasing the repetition frequency while maintaining a long pump duration will increase the risk of crystal damage. Therefore, we focused on the SSG when the pump duration was 2.2 ms at 150 Hz frequency. The measurement waveforms with 2.2 ms pump duration at 1 Hz and 150 Hz were also shown in Fig. 4(b). Two last peaks at 150 Hz pump frequency were shown here, and the measurement time lasted ~80 ms to obtain the intensity of unamplified signal. At 150 Hz frequency, the relative intensity of initial signal before the pump becomes higher than that at 1 Hz, because of the remaining population inversion induced by the last pump excitation and ETU effect in a three-level system. As a result, the SSG increased by a factor of ~2.4 (SSG = 7) compared with that at 1 Hz frequency and 30 W absorbed pump peak power, as shown in Fig. 3.

3.3. High-power laser amplification

Amplification performance of the Er:YAP amplifier with high-power seed injection was studied using the QCW oscillator. We specially focused on the amplification of single laser pulse. In this case, the maximum pulse energy of the seed laser injected into the Er:YAP amplifier was 4.2 mJ, and the peak power was calculated to be 3.2 W. The LD pump duration of the amplifier was set to be 2.2 ms. Meanwhile, the start time of the pump pulse was designed ~720 µs earlier than the seed laser pulse, i.e., slightly shorter than the fluorescence lifetime of $^4I_{11/2}$ level to increase the energy storage of the Er:YAP at the leading edge of the seed [20]. Figure 5(a) shows the typical temporal waveforms of the laser before and after the amplification at 30 W absorbed pump peak power. The noise signals in the seed were amplified, resulting in obvious sub-pulses in a main laser pulse. Besides, the trailing edge rather than the leading edge of the pulse was quickly amplified. This unusual phenomenon should be attributed to unsaturated amplification [27] as well as a higher gain with the pump time extending, as we have discussed in the SSG measurement. The nonuniform gain during the pump duration also leads to a slightly narrower pulse width, i.e., 1.2 ms after the amplification at 30 W absorbed pump peak power.
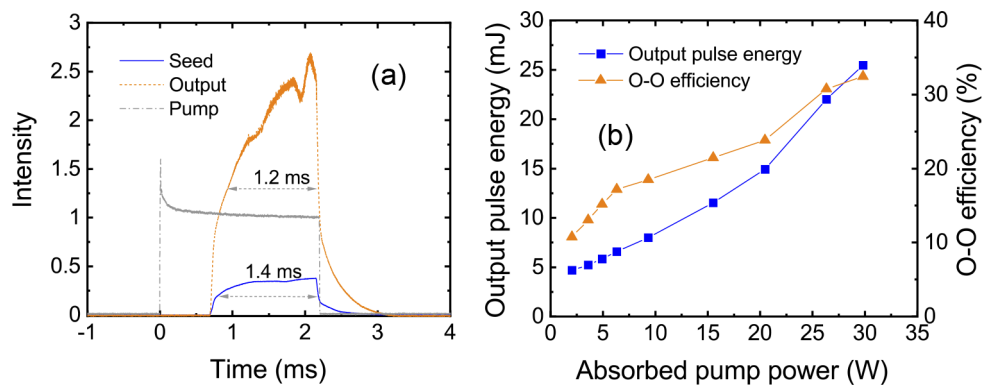
Fig. 5. Performance of high-power amplification. (a) Temporal waveforms before and after the amplification at 30 W absorbed pump peak power; (b) Output energy and O-O efficiency dependence on the absorbed pump peak power.

Figure 5(b) shows the dependence of the output pulse energy and O-O efficiency (extracted energy to the absorbed pump energy [28]) on the absorbed pump power. For the seed energy of 4.2 mJ and total absorbed pump peak power of 30 W, an output energy of 25.5 mJ was obtained from the amplifier, corresponding to an O-O efficiency of 32.3%, which indicates the feasibility of achieving high-efficiency amplification using Er:YAP crystal. The laser peak power after the amplification was calculated to be 21.8 W, corresponding to a peak power gain of ~6.8. Thus, it

can be ensured that the system was not saturated since the current gain was close to the SSG at the same pump peak power.

If ignoring the complex interactions between Er^{3+} ions, the saturation intensity I_s of a quasi-three-level system in the QCW mode can be given by [29]:

$$I_s = \frac{hv}{(1 + f_a/f_e)\sigma_e \tau_f} \tag{1}$$

where h is the Planck constant, v is the frequency of signal laser, f_a and f_e are Boltzmann's factors of stark levels of $^4I_{13/2}$ (0.064) and $^4I_{11/2}$ (0.204) for 2920 nm wavelength, respectively. σ_e is the effective emission cross-section at 2920 nm (3×10^{-20} cm^2) [20], and τ_f is the fluorescence lifetime (0.85 ms). Here we estimate the I_s using the measured average effective emission cross-section, which only has slight impact on the evaluation. According to Eq. (1), I_s could be calculated to be 2 kW/cm^2, which is much lower than the power density of 4.5 kW/cm^2 in our case. Therefore, the I_s of the Er:YAP amplifier has increased attributed to the ETU effect ($^4I_{13/2} + {}^4I_{13/2}$ $^4I_{15/2} + {}^4I_{9/2}$), since the inverted population density can be replenished continuously. Accordingly, it can be inferred that high-gain amplification is still feasible with a higher seed power injection.

4. Conclusion and outlook

In conclusion, we have successfully demonstrated an LD-pumped Er-doped solid-state MOPA system working at 2920 nm. Er:YAP crystal was employed as the gain medium in the MOPA system for the advantages of extremely high conversion efficiency with a low doping concentration. Both the characteristics of oscillator and amplifier were measured and discussed in detail. For the oscillator, increasing the pump frequency to ≥140 Hz to maintain the laser working at a three-level system can effectively suppress the generation of a giant pulse. While for the amplifier, SSG that close to the parasitic oscillation limit (SSG = 10.5) can be obtained at 1 Hz frequency with ≥10 ms pump duration, which proves that laser amplification using LD end-pumped Er:YAP amplifier is feasible. With 2.2 ms pump duration, the SSG was obviously improved at 150 Hz frequency compared with that at 1 Hz due to the enhanced ETU effect. In the final amplification experiment, 25.5 mJ of pulse energy was obtained with a peak power of 21.8 W. The O-O efficiency was as high as 32.3%, confirming the feasibility of power amplification with high conversion efficiency. Further achievement of power amplification at lower repetition frequency and longer pump duration may be possible by using an anti-reflection coated Er:YAP crystal in the amplifier stage, and an acousto-optic modulator to reduce the frequency of the seed laser outside the oscillator cavity. In addition, CW laser amplification is still possible through excellent heat management. We believe that our current results could be the guideline for the power improvement of mid-infrared lasers in the future.

Disclosures. The authors declare no conflicts of interest.

Data availability. Data underlying the results presented in this paper are not publicly available at this time but may be obtained from the authors upon reasonable request.

References

1. B. M. Walsh, H. R. Lee, and N. P. Barnes, "Mid infrared lasers for remote sensing applications," J. Lumin. **169**, 400–405 (2016).
2. M. C. Pierce, S. D. Jackson, M. R. Dickinson, T. A. King, and P. Sloan, "Laser-tissue interaction with a continuous wave 3 μm fiber laser: preliminary studies with soft tissue," Lasers Surg. Med. **26**(5), 491–495 (2000).
3. http://hitran.iao.ru/molecule.

4. G. M. Hale and M. R. Querry, "Optical constants of water in the 200 nm to 200 µm wavelength region," Appl. Opt. **12**(3), 555–563 (1973).
5. S. G. Prasad, A. De, and U. De, "Structural and optical investigation of radiation damage in transparent PET polymer films," Int. J. Spectrosc. **2011**, 1–7 (2011).
6. Y. O. Aydin, V. Fortin, R. Vallée, and M. Bernier, "Towards power scaling of 2.8 µm fiber lasers," Opt. Lett. **43**(18), 4542–4545 (2018).
7. K. Karki, V. Fedorov, D. Martyshkin, and S. Mirov, "High energy (0.8 J) mechanically Q-switched 2.94 µm Er:YAG laser," Opt. Express **29**(3), 4287–4294 (2021).
8. X. Ye, X. Xu, H. Ren, B. Zhang, Y. Lu, X. Chen, L. Zhang, X. Wei, M. Wan, and T. He, "Enhanced high-slope-efficiency and high-power LD side-pumped Er:YSGG laser," Appl. Opt. **58**(36), 9949–9954 (2019).
9. W. Yao, H. Uehara, H. Kawase, H. Chen, and R. Yasuhara, "Highly efficient Er:YAP laser with 6.9 W of output power at 2920 nm," Opt. Express **28**(13), 19000–19007 (2020).
10. W. Yao, H. Uehara, S. Tokita, H. Chen, D. Konishi, M. Murakami, and R. Yasuhara, "LD-pumped 2.8 µm Er:Lu2O3 ceramic laser with 6.7 W output power and >30% slope efficiency," Appl. Phys. Express **14**(1), 012001 (2021).
11. M. Pollnau, T. Graf, J. E. Balmer, W. Lüthy, and H. P. Weber, "Explanation of the cw operation of the Er^{3+} 3 µm crystal laser," Phys. Rev. A **49**(5), 3990–3996 (1994).
12. S. Georgescu and O. Toma, "Er:YAG three-micron laser: performance and limits," IEEE J. Sel. Top. Quantum. Electron. **11**(3), 682–689 (2005).
13. B. J. Dinerman and P. F. Moulton, "3 µm cw laser operation in erbium-doped YSGG, GGG, and YAG," Opt. Lett. **19**(15), 1143–1145 (1994).
14. H. Uehara, S. Tokita, J. Kawanaka, D. Konishi, M. Murakami, S. Shimizu, and R. Yasuhara, "Optimization of laser emission at 2.8 µm by Er:Lu$_2$O$_3$ ceramics," Opt. Express **26**(3), 3497–3507 (2018).
15. H. Uehara, D. Konishi, K. Goya, R. Sahara, M. Murakami, and S. Tokita, "Power scalable 30 W mid-infrared fluoride fiber amplifier," Opt. Lett. **44**(19), 4777–4780 (2019).
16. G. Zhu, X. Zhu, R. A. Norwood, and N. Peyghambarian, "Experimental and numerical investigation on Q-switched laser-seeded fiber MOPA at 2.8 µm," J. Lightwave Technol. **32**(23), 4553–4557 (2014).
17. S. Duval, J. Gauthier, L. Robichaud, P. Paradis, M. Olivier, V. Fortin, M. Bernier, M. Piché, and R. Vallée, "Watt-level fiber-based femtosecond laser source tunable from 2.8 to 3.6 µm," Opt. Lett. **41**(22), 5294–5297 (2016).
18. N. M. Wannop, M. R. Dickinson, and T. A. King, "An erbium:YAG oscillator-amplifier laser system," Opt. Commun. **113**(4-6), 453–457 (1995).
19. A. Joshi, M. Furtado, R. Shori, and O. M. Stafsudd, "Small-signal gain measurement for highly doped and co-doped Er^{3+}:YAG at 2.936 µm," Opt. Laser Technol. **56**, 58–64 (2014).
20. H. Kawase and R. Yasuhara, "2.92 µm high-efficiency continuous-wave laser operation of diode-pumped Er:YAP crystal at room temperature," Opt. Express **27**(9), 12213–12220 (2019).
21. M. Stalder and W. Lüthy, "Polarization of 3 µm laser emission in YAlO$_3$:Er," Opt. Commun. **61**(4), 274–276 (1987).
22. Y. Sang, D. Liu, X. Xia, B. Zhang, P. Wang, Y. Chen, Z. Xu, W. Liu, J. Guo, and F. Sang, "A multi-wavelength pulsed mid-infrared laser based on Er:YAG," Opt. Commun. **485**, 126667 (2021).
23. H. Uehara, R. Yasuhara, S. Tokita, J. Kawanaka, M. Murakami, and S. Shimizu, "Efficient continuous wave and quasi-continuous wave operation of a 2.8 µm Er:Lu$_2$O$_3$ ceramic laser," Opt. Express **25**(16), 18677–18684 (2017).
24. L. Gomes, A. F. H. Librantz, F. H. Jagosich, W. A. L. Alves, I. M. Ranieri, and S. L. Baldochi, "Energy transfer rates and population inversion of ${}^4I_{11/2}$ excited state of Er^{3+} investigated by means of numerical solutions of the rate equations system in Er:LiYF$_4$ crystal," J. Appl. Phys. **106**(10), 103508 (2009).
25. A. K. Sridharan, S. Saraf, S. Sinha, and R. L. Byer, "Zigzag slabs for solid-state laser amplifiers: batch fabrication and parasitic oscillation suppression," Appl. Opt. **45**(14), 3340–3351 (2006).
26. H. Furuse, J. Kawanaka, N. Miyanaga, T. Saiki, K. Imasaki, M. Fujita, K. Takeshita, S. Ishii, and Y. Izawa, "Zig-zag active-mirror laser with cryogenic Yb^{3+}:YAG/YAG composite ceramics," Opt. Express **19**(3), 2448–2455 (2011).
27. W. Koechner, *Solid-State Laser Engineering* (VI ed., Springer, 2006), Chap. 4.
28. D. Creeden, B. R. Johnson, G. A. Rines, and S. D. Setzler, "High power resonant pumping of Tm-doped fiber amplifiers in core- and cladding-pumped configurations," Opt. Express **22**(23), 29067–29080 (2014).
29. T. Y. Fan and R. L. Byer, "Diode laser-pumped solid-state lasers," IEEE J. Quantum Electron. **24**(6), 895–912 (1988).